buildings

MDPI

Article

Metal-Nails Waste and Steel Slag Aggregate as Alternative and Eco-Friendly Radiation Shielding Composites

Mohammed M. Attia [1,*], Bassam Abdelsalam Abdelsalam [1], Mohamed Amin [1], Ibrahim Saad Agwa [1,2] and Mohammad Farouk Abdelmagied [3]

[1] Civil and Architectural Constructions Department, Faculty of Technology and Education, Suez University, Suez 43713, Suez, Egypt; bassam.abdelsalam@suezuniv.edu.eg (B.A.A.); h_scc@yahoo.com (M.A.); ibrahim.agwa@suezuniv.edu.eg (I.S.A.)
[2] Civil Engineering Department, El-Arish High Institute for Engineering and Technology, El-Arish 45511, North Sinai, Egypt
[3] Civil Engineering Department, Benha Faculty of Engineering, Benha University, Benha 13511, Qalyubiyya, Egypt; dr.mohamed.farouk@bhit.bu.edu.eg
* Correspondence: mohammed.mahmoudattia@suezuni.edu.eg

Abstract: Metal waste recycling has become a global requirement owing to its environmental benefits and powerful economic activity. Metal nail waste (MNW) is a byproduct of metal nail manufacture. MNW has an equal size, contains a high ratio of iron, and has a high specific gravity comparable to normal aggregate. We present MNW recycling as a partial replacement for fine aggregates and electric arc furnace steel slag (EAFSS) as coarse aggregates to produce sustainable heavyweight concrete (HWC). Our main research aim was to study the radiation shielding and mechanical properties of sustainable HWC by partially replacing MNW with 10, 20, 30, and 40% sand. EAFSS is a coarse aggregate for 60% of the total volume. Fresh and hardened properties of HWC are presented. Furthermore, we analysed the internal structure of HWC mixes using a scanning electron microscope. Our results showed the positive effects of MNW on the unit weight of concrete. The density of HWC mixes ranges between 2650 and 3170 kg/m^3. In addition, MNW contributes to increasing the compressive strength of concrete mixes with their use of up to 30%. Therefore, the MNW ratios improved the failure behaviour of HWC mixes. The improved linear attenuation coefficient of HWC mixes was due to using MNW ratios and higher densities than the reference mix.

Keywords: electric arc furnace steel slag; heavyweight concrete; mechanical properties; metal nails waste; radiation shielding; sustainable concrete

Citation: Attia, M.M.; Abdelsalam, B.A.; Amin, M.; Agwa, I.S.; Abdelmagied, M.F. Metal-Nails Waste and Steel Slag Aggregate as Alternative and Eco-Friendly Radiation Shielding Composites. *Buildings* **2022**, *12*, 1120. https://doi.org/10.3390/buildings12081120

Academic Editor: Haoxin Li

Received: 17 June 2022
Accepted: 25 July 2022
Published: 29 July 2022

1. Introduction

Concrete is the most commonly used material in the construction industry because of its availability, durability, and low cost [1–3]. The EN 206-1 specification indicates that concrete is considered heavyweight concrete HWC with a dry specific gravity >2600 kg/m^3 [4–7]. The most common aggregates to produce HWC are limonite, hematite, magnetite, ilmenite, and barite [8,9]. HWC is widely used for radiation protection in industrial, medicinal, and research applications [10], leading to the consumption of raw natural heavyweight aggregates [4,5]. However, the availability of natural heavyweight aggregates is decreasing due to high demand, leading to an increased need for alternative sources [11]. Although the HWC is more suitable for radiation shielding, the production of HWC is expensive. Waste materials such as recycled aggregates of lead waste, copper slag, steel slag, etc., present good radiation shielding and reduce costs [12,13].

According to the United Nations' World Commission on Environment and Development, sustainability means "meeting the needs of the present without compromising the ability of the future generations to meet their own needs" [14]. Therefore, managing materials sustainably necessitates paying attention to a product's whole life cycle, from the time

it was manufactured through its usage and eventual recycling or disposal. Sustainability Materials Management is the term for this initiative [15,16]. The concrete industry has implemented several strategies to meet these objectives in response to mounting environmental pressure to decrease waste and pollution and recycle as much as possible [17]. It is necessary to critically evaluate the methods, practices, and raw material sources currently used in construction so that natural and industrial wastes and by products, which formerly received little to no attention, become prominent [18].

The aggregates represent a minimum of three-quarters of the concrete volume; coarse and fine aggregates comprise around 40–50 and 20–30%, respectively, of the hardened concrete's total volume. They are used to reduce costs, shrinkage, and creep and increase the mechanical strength of concrete. They are typically inert, and their properties affect those of concrete [8,19]. Therefore, assuring the supply of high-quality aggregates is crucial for building concrete. In addition, the aggregate should also be economical, sustainable, and environmentally friendly [20]. Reusing industrial solid waste as a partial aggregate replacement in construction projects frees up landfill space and lessens the need to mine natural raw materials. This strategy ensures enough resources for future generations and achieving sustainable development calls for the preservation of natural aggregates [21].

The annual production of ferrous materials worldwide has increased to over 60% in the last decade, amounting to approximately 1300 million tons. Steel slag is a by-product of steel manufacturing. The production of one ton of steel yields 130–200 kg of slag, according to the composition of and process of steel production [22,23]. The common chemical compounds in steel slag are SiO_2, CaO, Fe_2O_3, Al_2O_3, and MnO. The major mineral components of steel slag are C_3S, C_2S, C_4AF, R_O phase, and free-CaO [24]. This by-product (consisting mainly of calcium carbonate) is divided into small sizes. These products are used as aggregates in concrete production. For example, the annual steel production in China was internationally rated first, with nearly 740 million tons of steel slag generated in 2009 [25]. The compressive strength of cement concrete is significantly influenced by the pace at which steel slag aggregate is substituted. Miah et al. [26] found that the compressive strength increased with the augmentation of slag aggregate replacement rates by 28.46, 42.67, and 55.89%, respectively, when used to replace 40, 60, and 80% of coarse aggregate. Saxena and Tembhurkar [27] reported that compressive strength reached its maximum value when steel slag replaced 50% of coarse aggregate. Wang et al. investigated the splitting tensile and flexural strength of concrete using coarse steel slag aggregate [28]. Their test findings demonstrated that slag aggregate concrete's splitting tensile strength in 28 days was greater than the control group at higher replacement rates (75 and 100%).

One of the main components of industrial solid waste in Egypt is iron. Small- and medium-sized workshops and iron and steel manufacturing facilities are anticipated to be the main suppliers of this kind of solid waste. Although there are no accurate statistics on these waste amounts produced in Egypt, there are unmistakable indications of a sharp rise in the total amount discarded as solid wastes due to the absence of or subpar operation systems for the collection, treatment, and disposal of these wastes. Better radiation resistance by HWC is produced by heavy metal because it contains a high percentage of ferrous elements [29,30]. Ghailan [31] used industrial solid waste produced by the iron and steel industry and found that concrete mixes produced from waste material performed better than conventional concrete mixes. Ismail and Al-Hashmi [32] also noted improvements in compressive and flexural strength when waste iron was substituted for 20% of the sand compared to references. Other researchers discovered that concrete with iron filings had better compressive strength than regular concrete. Additionally, iron filings increase concrete's ductility [33].

In this study, to achieve the term sustainability, metal waste materials were used as an alternative to sand as fine aggregates, whereas steel slag was used (rather than dolomite) as coarse aggregates to produce sustainable HWC. Therefore, the main objective of our study was to measure the linear attenuation coefficient of HWC with MNW portions, then calculate half, tenth-value layers, and the mean free path (HVL, TVL, and Mfp).

In addition, we also aimed to determine the unit weight, compressive strength, tensile strength, modulus of elasticity, and radiation properties of HWC mixes. Moreover, the microstructure of HWC mixes containing metal nail waste (MNW) ratios was analysed by scanning electron microscope (SEM).

2. Experimental Procedure

2.1. Materials

We used ordinary Portland cement (OPC) CEM I 42.5N in our research. OPC conforms to the requirements of the specification discussed in [34]. A total of 15% limestone powder (LSP) was used as additive content to cement. The LSP originated from crushed stone in Attaka, Suez, Egypt. The properties of LSP were 2250 cm^2/g and 2.60 for specific area and gravity, respectively. LSP was added to the HWC mixture to enhance the fresh properties of concrete and avoid aggregate segregation into the concrete mix.

MNW is a metal waste byproduct gathered from metal nails manufactured by the Elmasry group company (Egypt). This waste is washed in gasoline to remove oil from the MNW surface and then left to dry before using it in concrete. Waste particles were graded using sieve analysis to replace sand as a fine aggregate. Semi-quantitative analysis was conducted for MNW using energy-dispersive X-ray (EDX) spectroscopy. The EDX analysis results showed the atomic ratios of each element in MNW, as shown in Figure 1.

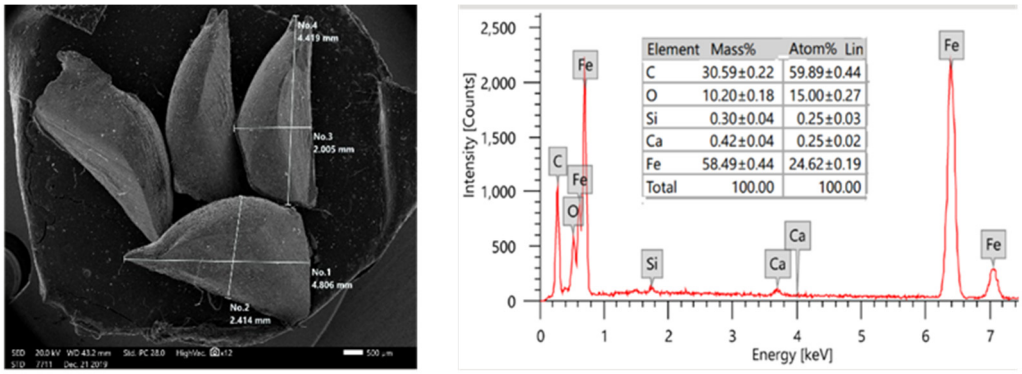

Figure 1. EDX analysis of MNW.

MNW contains 59% iron (Fe), which is classified as heavyweight material compared to sand (normal weight aggregate). MNW was altered by the sand content with ratios of 10, 20, 30, and 40%. EAFSS was used as a heavyweight coarse aggregate and produced during the manufacturing of crude EAFSS and steel by the Suez steel company in Egypt. EAFSS is a strong, dense, safe, and durable aggregate; it is cube-shaped with good resistance to deformation. The particle sizes of MNW and EAFSS aggregates are shown in Figure 2. A sieve analysis test was performed on fine and coarse aggregates in accordance with [35], as shown in Figure 3. The fine to coarse aggregate ratio was 40:60%, respectively. Table 1 presents the physical properties of fine and coarse aggregates.

Table 1. Physical properties of fine and coarse aggregates.

Properties	Fine Aggregate		Coarse Aggregate
	Sand	MNW	EAFSS
Bulk density (t/m^3)	1.65	6.30	1.99
Specific gravity	2.65	5.50	3.50
Water absorption (%)	2.50	0.20	1.02
Los Anglos abrasion loss (%)	18.50	3.00	14.1

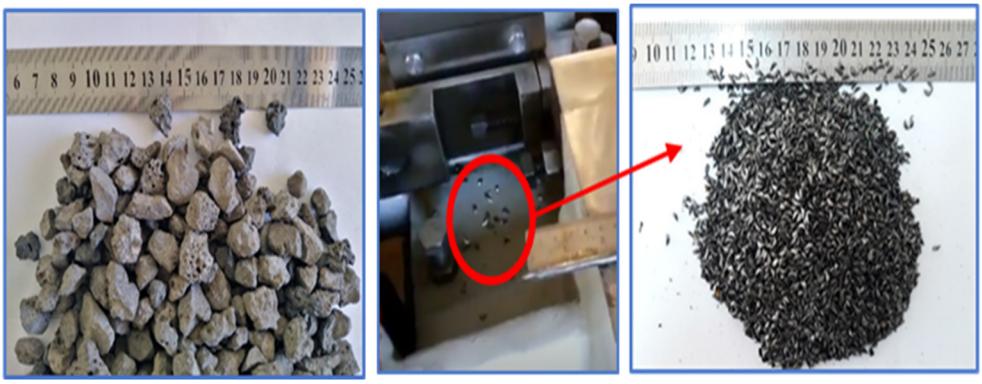

(**a**) (**b**)

Figure 2. Particle size of fine and coarse aggregates. (**a**) EAFSS. (**b**) MNW.

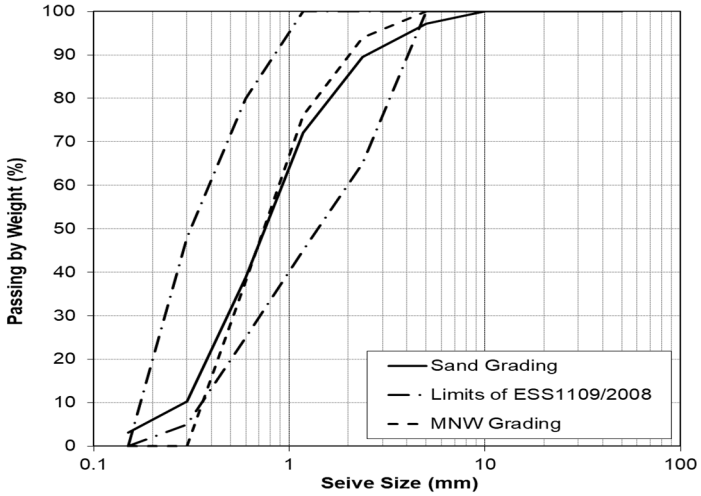

(**a**)

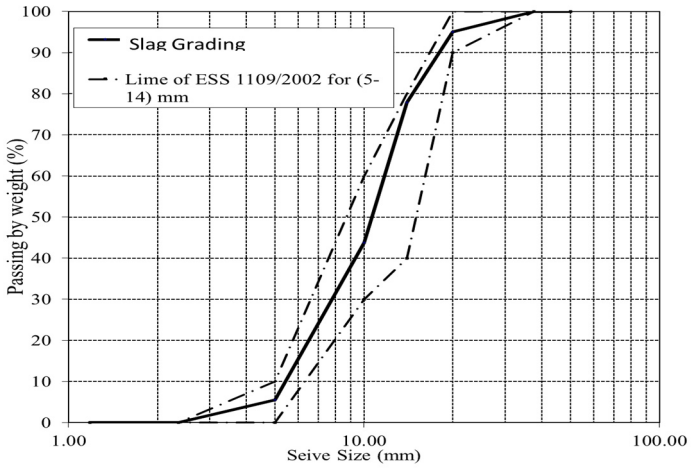

(**b**)

Figure 3. Sieve analysis of fine and coarse aggregates. (**a**) Fine aggregate (sand and MNW). (**b**) Coarse aggregate (EAFSS).

Anti-washout admixtures (AWA) were used to create homogenous mixture components and prevent the segregation of HWC ingredients. AWA maintains the flowability mixes' cohesive nature owing to the presence of a powder base. Superplasticizer was added to reduce water content and improve the workability of fresh concrete. Viscocrete-5930 has

a specific gravity of 1.11 and was added to the mixture with ratios between 2 and 2.8%. Viscocrete-5930 was acceptable according to ASTM specifications [36].

2.2. Mix Proportion

Five mixes were experimented with in this study to produce HWC. The replacement ratios of MNW were 0, 10, 20, 30, and 40% as fine aggregates from sand content. Superplasticizer percentages were used (ranging between 2.0 and 2.8% from cement content) to maintain the HWC mixes' good workability. The water-to-binder ratio was constant with 0.4 from cementitious content. The mixture proportions for each mix are tabulated in Table 2. The following procedures describe the mixing steps of HWC. Firstly, fine and coarse aggregates, such as sand and EAFSS, were continuously stirred in a mixing pan in dry conditions for 3 min. Secondly, fine materials, such as cement and LSP, were added to the aggregate and constantly mixed thereafter for 5 min. Thirdly, MNW was added to mix, and all components were mixed for 3 min to become even more homogenous. Lastly, water, superplasticizer and AWA were added, and the mix was stirred for 2 min before being cast in moulds.

Table 2. Concrete mixtures proportions (kg/m^3).

Mixes ID	Cement	LSP	Aggregates			AWA	Superplasticizer	w/b
			Fine		Coarse			
			Sand	MNW	EAFSS			
M-0	450	67.5	750	0	1125	0.45	9.0	207
M-10	450	67.5	675	156	1252	0.45	9.9	207
M-20	450	67.5	600	311	1252	0.45	11.2	207
M-30	450	67.5	525	467	1252	0.45	11.7	207
M-40	450	67.5	450	623	1252	0.45	12.6	207

2.3. Testing Procedure

The slump test was performed considering [37]. A cubic specimen with dimensions of 150 mm was designated for the compressive strength test at 7 and 28 in accordance with [38]. According to ASTM classifications, the splitting tensile and modulus of elasticity tests were conducted at 28 d on cylinder samples (150 × 300 mm) [39,40]. The microstructure of the HWC specimens was obtained through SEM analysis at 28 d.

Two gamma-ray sources, ^{137}Cs and ^{60}Co, with photon energies of 0.66 and 1.33 MeV, respectively, were used for the attenuation test at 28 days. The test specimens had dimensions with a surface area of 10 × 10 cm with a thickness ranging from 2 to 8 cm. Before testing, the samples were cured and then dried in an oven at 105 °C. The transmitted intensity (I) was calculated based on the Beer–Lambert law, as shown in Equation (1) [41]. We also calculated the total mass attenuation coefficient (μm), as presented in Equation (2) [42].

$$I = I_o e^{-\mu x} \quad (1)$$

$$\mu m = \mu / \rho \quad (2)$$

where:

x: Sample thickness (cm);
I_o: Source intensity;
μ: Linear attenuation coefficient;
ρ: Sample density.

The half value layers (HVL), tenth value layers (TVL) and mean free path (Mfp) were calculated as exhibited by Equations (3)–(5) [43,44]. These measurements were measured at the gamma-ray sources and photon energies mentioned previously. These calculations show that the radiation intensity reduces compared with the initial intensity.

$$HVL = \ln 2/\mu \quad (3)$$

$$TVL = \ln 10/\mu \quad (4)$$

$$Mfp = 1/\mu \quad (5)$$

3. Experimental Results and Discussions

3.1. Fresh Concrete Properties

The slump test is the initial factor worth considering for concrete workability. The slump values were 140, 135, 125, 120, and 110 mm for HWC mixes containing 0, 10, 20, 30, and 40% of MNW, respectively. The slump decreased with the increased MNW replacement ratios from the sand. With respect to the control mix, the reduction percentages of MNW mixes with replacement ratios of 10, 20, 30, and 40% were 4, 11, 15, and 22%, respectively. Similar to the findings of [32], which show that when waste-iron ratios are increased by 20% in concrete mixes and it is utilized as a replacement for sand, slump tests decrease by 10%. The reduced workability is attributed to MNW replacing sand. Moreover, the void ratios in the concrete mixes, which possessed fine MNW, were substantially higher than that of concrete and possessed natural sand. Furthermore, this tendency may be related to MNW's heterogeneity and angular forms, which cause concrete mixtures to be less fluid. Therefore, an additional superplasticizer was used to achieve acceptable workability for HWC.

3.2. Hardened Concrete Properties

3.2.1. Unit Weight

We determined that the unit weight of concrete complied with the ASTM C138/C138M-17a specifications [45]. According to [7], HWC is defined as having a dry density greater than 2600 kg/m^3. Figure 4a illustrates the unit weight of the different HWC mixes, with each value of the listed unit weight being the average of three samples. At 28 days, the unit weight of HWC mixtures was recorded from 2650 kg/m^3 to 3170 kg/m^3. The unit weight of control mix M-0 shows a heavyweight mixture of 2650 kg/m^3 due to using EAFSS as the coarse aggregate; the fine to coarse aggregates ratio was 1:1.5. Once MNW was used as a fine aggregate with different percentages, the unit weight of the concrete increased. The unit weights were 2790, 2925, 3020, and 3170 kg/m^3 for M-10, M-20, M-30, and M-40, respectively. The high unit weight of the concrete mixes may be attributed to the higher bulk, specific gravity, and unit weight of MNW than sand, as seen in Table 1. However, HWC depends on high weight components and properties. EAFSS, as a coarse aggregate, and MNW, replaced by sand with 10, 20, 30, and 40%, contributed to producing HWC.

3.2.2. Compressive Strength

The compressive strength of HWC was determined by the average of three cubes from each concrete mix. Figure 4b presents the compressive strength results at 7 and 28 days. The compressive strength at 7 days of HWC mixes was 42.9, 44.1, 47, 48.2, and 39 MPa for mixes M-0, M-10, M-20, M-30, and M-40, respectively. The increment ratio was 2.8, 9.6, and 12.4% for mixes using 10, 20, and 30% MNW compared to the control mix M-0. The compressive strength at 28 days of HWC mixes was 55.3, 55.8, 57, 61.3, and 54.5 MPa for mixes M-0, M-10, M-20, M-30, and M-40, respectively. The compressive strength results revealed high-strength concrete according to [46]. The mixtures M-10, M-20, and M-30 exhibited higher compressive strength at 28 days than the control mix M-0 by 1, 3.1, and 10.9%, respectively. These results may be due to the MWN aggregate's high density and strength [47]. Ismail and Al-Hashmi [32] studied waste iron's impact on concrete characteristics. Their findings showed that waste iron-based concrete mixtures had higher compressive strengths than normal concrete mixes.

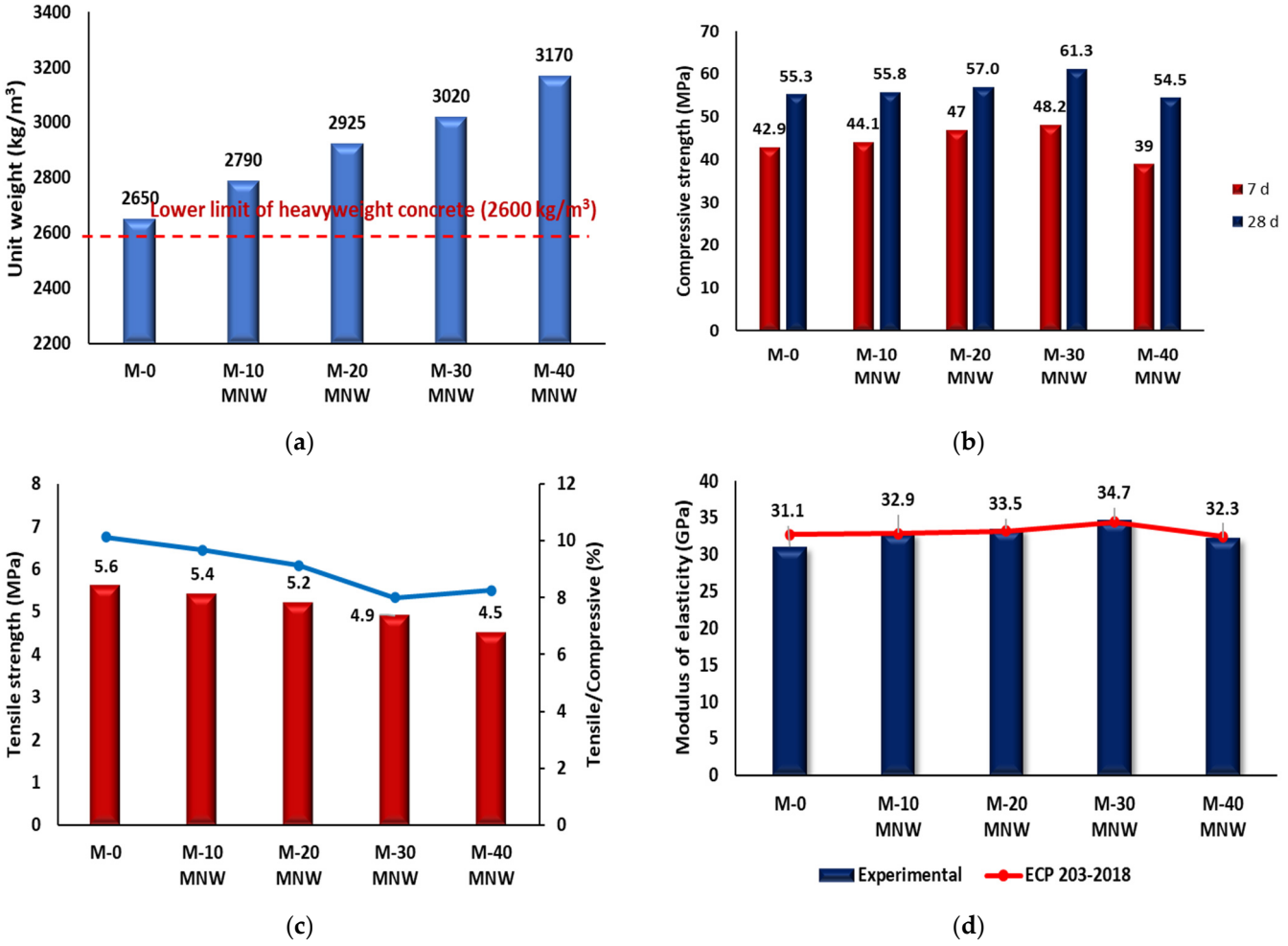

Figure 4. (**a**). Unit weight of all mixtures at 28 d; (**b**) compressive strength of all mixtures at 7, 28 d; (**c**) tensile strength of all mixtures at 28 d; (**d**) modulus of elasticity for all mixtures at 28 d.

The compressive strength of HWC increased with increased curing ages by about 27% at 7 days. This increase is attributed to increased hydration products, particularly berm rite gel, leading to increased compressive strength. Although sand generally acts as a reinforcement in cementitious composite matrices, the concrete can break down under compressive loading in the presence of sand particles. This aspect explains the incoherency between sand surfaces and the formed C-SH, further causing a fracture and crack propagation [48]. In addition, using up to 30% MNW contributes to improved compressive strength for HWC mixtures. Mohamed Alwaeli et al. [49] discovered that replacing sand with up to 25% steel scrap increased compressive strength. However, MNW exceeding 30% decreases the compressive strength of HWC mixes by 1.5% of M-0, which may be due to MWN accumulating on cement particles and producing a pseudomorph layer with low penetration [50]. However, this leads to weaker bonding forces between cement and steel waste than between cement and sand [48].

Finally, Tufekci et al. [51] studied the effects of fine aggregates (silica sand and quartz powder blend (REF), granulated ferrous waste (GFW), and barite sand (BAR)) on compressive strength. The series produced with GFW fine aggregate achieved the highest compressive strength compared with other series, confirming the direction of the results.

3.2.3. Tensile Strength

The indirect tensile strength of HWC mixes was 5.6, 5.4, 5.2, 4.9, and 4.5 MPa for mixtures M-0, M-10, M-20, M-30, and M-40, respectively. The reduction ratios of tensile strength were 3.6, 7.1, 12.5, and 19.6% for mixes using 10, 20, 30, and 40% MNW compared to the control mix. Figure 4c shows the splitting tensile strength results for all mixes at 28 days, which possessed the replacement ratios of MNW as fine aggregates. The HWC mixes containing 10, 20, 30, and 40% MNW had lower tensile strengths than the control mix, with reduction ratios between 3.6 and 19.6%. The reduction in tensile strength for HWC mixes may be due to the lack of bonding at the smooth surface of the interfacial transition zone (ITZ) between the cement paste and MNW particles. Furthermore, this may cause an accumulation of iron particles preventing water from penetrating the cement and slowing its hydration [32]. We calculated the tensile/compressive ratio, which ranged between 8 and 10% of the compressive strength result for each HWC mix, as presented in Figure 4c. MNW enhanced the issue of sudden failure for HWC cylinders due to the good MNW distribution in the mix, as shown in Figure 5. The cylinder without MNW split into two half-cylinders, whereas the cylinder with MNW exhibited no separation after reaching the maximum tensile strength [52].

Figure 5. Effects of MNW on failure mode and distribution shape in concrete. (**a**) Failure mode due to tensile test. (**b**) Distribution shape of MNW.

3.2.4. Elasticity Modulus

According to the American Concrete Institute, the modulus of elasticity in concrete is an important test to achieve structural concrete requirements [53]. Figure 4d illustrates the influence of MNW volume fractions on the modulus of elasticity in HWC. The test results showed that the modulus of elasticity in HWC increased by 5.80% when MNW increased from 0 to 10%, 14.15% from 0 to 20%, 11.58% from 0 to 30%, and 3.90% from 0 to 40%. The maximum value of the modulus of elasticity in all mixes was 35.5 GPa at 20% MNW.

4. SEM Analysis

Figure 6a presents SEM images of the control mixture (M-0). EAFSS would wedge into the concrete mix along with the formation, which is effective in terms of material cohesion. Figure 6b–e shows the present SEM images ITZ of MNW in cement paste for the mixture (M-10 MNW, M-20 MNW, M-30 MNW, and M-40 MNW) replacement levels of the microstructures compared to those in the control. Figure 6c, d shows that MNW ratios contribute to an increase in its compressive strength of HWC mixtures up to using 30% MNW. Accordingly, the rough surface of MNW may increase adhesion to the cement paste, thereby increasing compressive strength. However, Figure 6e shows that the MNW ratios decrease with the compressive strength of the concrete mixture (M-40 MNW). Consequently, an increase of over 30% MNW may hinder adhesion to the cement paste, thereby reducing compressive strength.

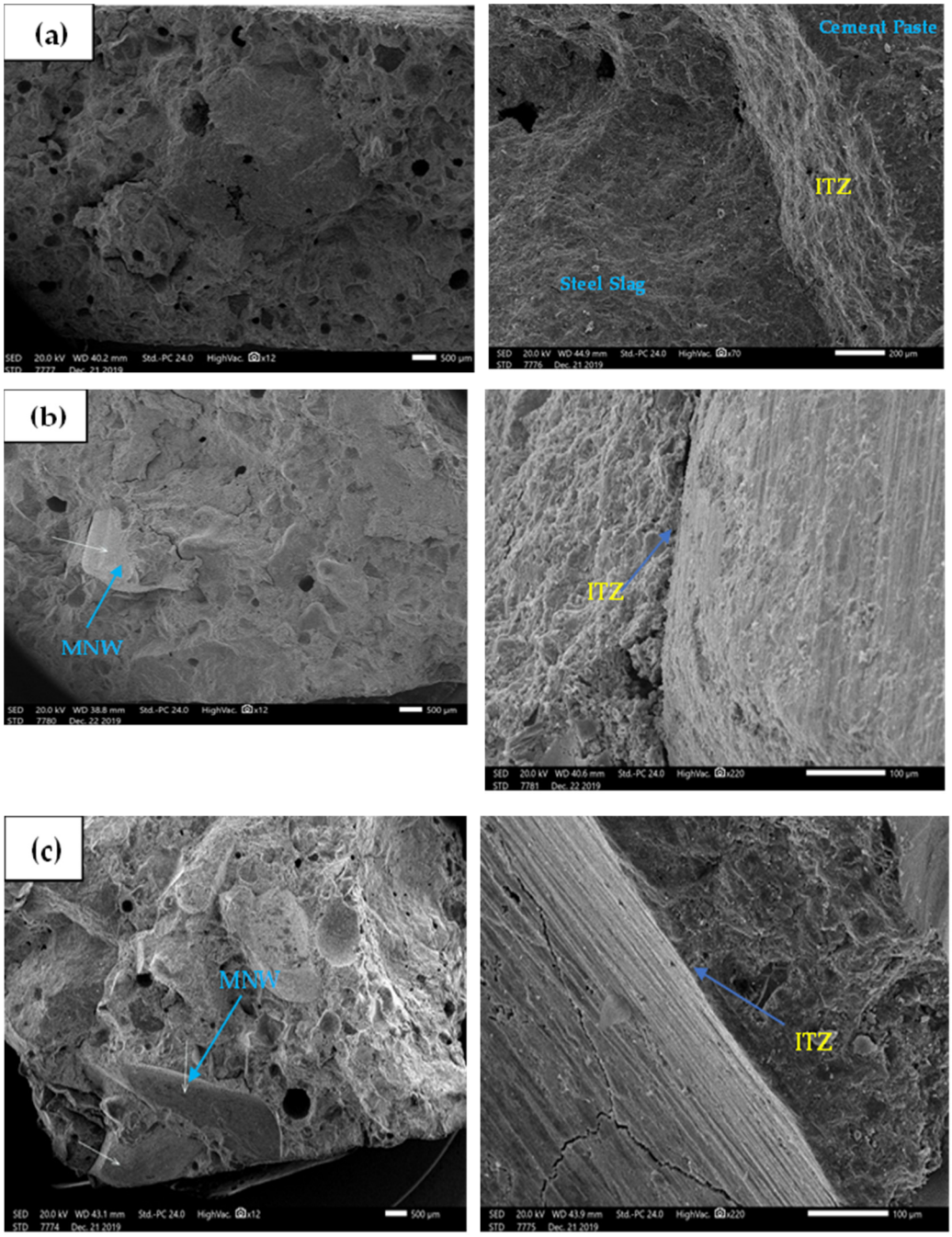

Figure 6. *Cont.*

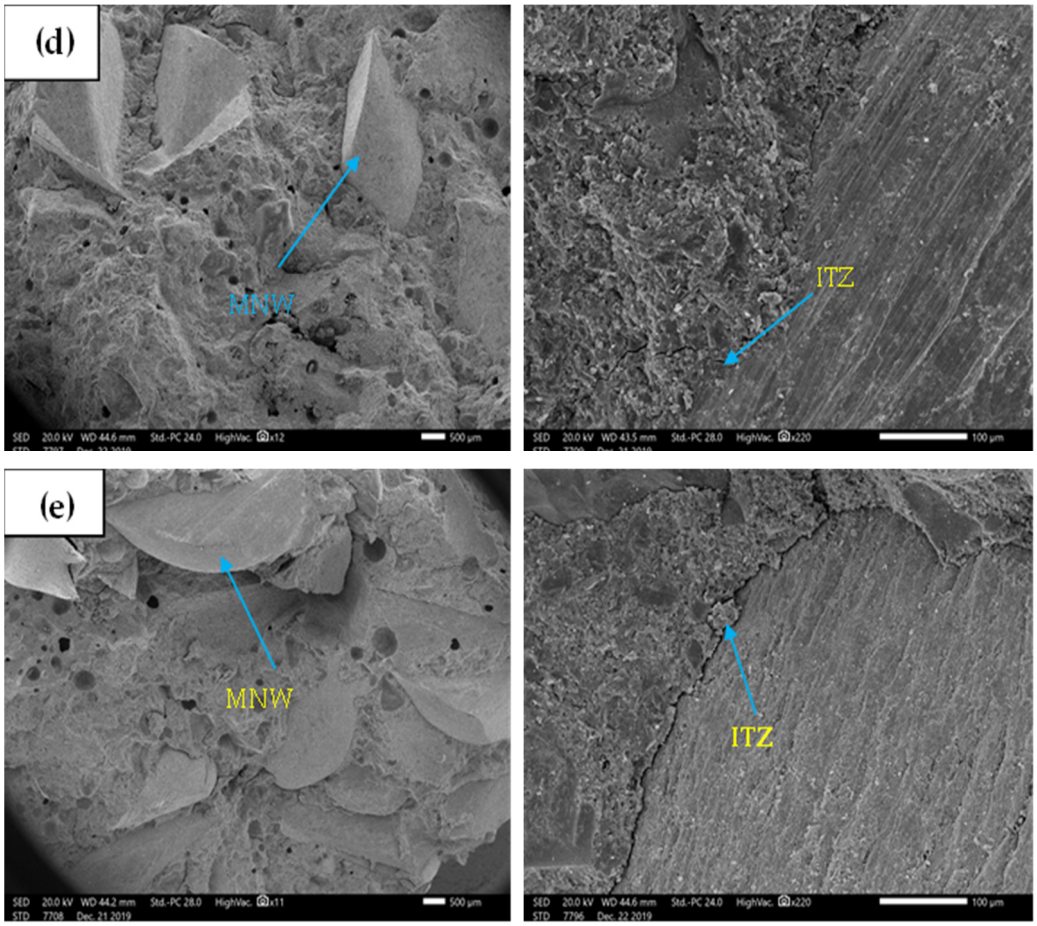

Figure 6. SEM images ITZ of MNW in cement paste: (**a**) M-0; (**b**) M-10MNW; (**c**) M-20MNW; (**d**) M-30MNW; (**e**) M-40MNW.

5. Radiation Properties

In this study, we measured the radiation properties μ, μm, HVL, TVL, and Mfp for HWC mixtures produced with MNW; the results are shown in Table 3. The improved linear attenuation coefficient of HWC mixes is due to using MNW ratios and higher densities than the reference mix M-0, similar to the results reported in the studies of [54–57]. The increased ratios were 8.8, 16.9, 24.3, and 32.4% for M-10 MNW, M-20 MNW, M-30 MNW, and M-40 MNW, respectively, at a photon energy of 0.66 MeV for ^{137}Cs. By contrast, when subjected to a photon energy of 1.33 MeV for ^{60}Co, the enhanced percentages were 12.1, 22, 28.6, and 38.5% for mixes using 10, 20, 30, and 40% MNW, respectively. The attenuation coefficient development of sustainable HWC mixes is presented in Figure 7. From these linear attenuation coefficients, MNW contributes to the reduced thickness of HWC samples from 4.683 to 3.536 cm for HVL and 15.558 to 11.748 cm for TVL. The increased MNW ratios in HWC mixes led to attenuated energy due to MNW with 59% iron (Fe), as presented in the EDX analysis in Figure 1. The mean free path of HWC mixes reduced the distance between two successive interactions of photons by adding MNW portions. Figure 8 presents the thickness of HWC mixes at a photon energy of 0.66 MeV for ^{137}Cs.

Table 3. Radiation properties of HWC mixtures produced with MNW.

Mixes ID	Unit Weight (g/cm^3)	Gamma-ray Source	μ (cm^{-1})	μm (cm^2/g)	HVL (cm)	TVL (cm)	Mfp (cm)
M-0	2.650	^{137}Cs	0.148	0.056	4.683	15.558	6.757
M-10	2.790		0.161	0.058	4.305	14.302	6.211
M-20	2.925		0.173	0.059	4.007	13.310	5.780
M-30	3.020		0.184	0.061	3.767	12.514	5.435
M-40	3.170		0.196	0.062	3.536	11.748	5.102
M-0	2.650	^{60}Co	0.091	0.034	7.617	25.303	10.989
M-10	2.790		0.102	0.037	6.796	22.574	9.804
M-20	2.925		0.111	0.038	6.245	20.744	9.009
M-30	3.020		0.117	0.039	5.924	19.680	8.547
M-40	3.170		0.126	0.040	5.501	18.274	7.937

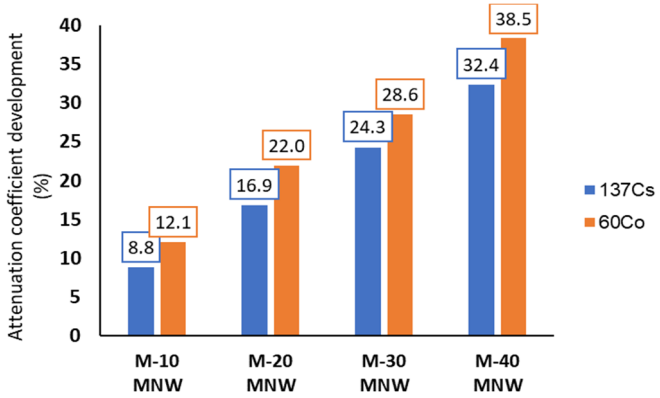

Figure 7. Attenuation coefficient (μ) development of sustainable HWC mixes.

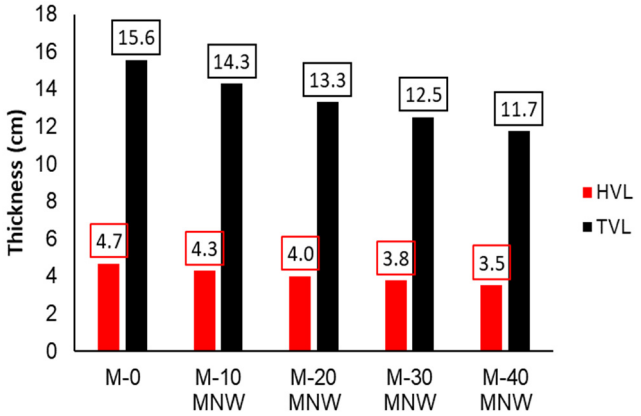

Figure 8. Thickness of HWC mixes at a photon energy of 0.66 MeV for ^{137}Cs.

6. Conclusions

This study used metal-nail waste as a partial replacement for sand to improve the compressive strength and gamma radiation attenuation of concrete. Metal-nail waste was used considered specifically for its high density, allowing it to be used as heavy aggregates. The results of this study are summarised as follows:

- The slump value of fresh concrete decreased with an increase in replacement ratios of the MNW by fine aggregates in HWC. The reduction percentages of the MNW mixes with replacement ratios of 10, 20, 30, and 40% were 4, 11, 15, and 22%, respectively,

compared to the reference mix without MNW. However, the workability of concrete was unaffected since the lowest slump value of the mixture was 110 mm with 40% MNW.

- All concrete mixes showed heavyweight concrete with values higher than 2600 kg/m^3 as indicated in specification EN 206/1. The unit weight increased using the MNW replacement ratios. MNW (0.0–0.40%) was changed by the weight of fine aggregate, in which the average unit weight was approximately 2650 to 3170 kg/m^3.
- The replacement ratio of 30% MNW is the maximum percentage of waste that can partially replace the conventional aggregates in concrete production. The MNW ratios improved the compressive strength of the concrete mixtures up to a 30% MNW replacement ratio from fine aggregates, which showed a higher value of 10.9%.
- The reduction ratios of tensile strength were 3.6, 7.1, 12.5, and 19.6% for mixes using 10, 20, 30, and 40% MM compared to the control mix. On the other hand, the failure behaviour of HWC mixes was enhanced using MNW ratios. The HWC cylinder without MNW split into two half-cylinders. By contrast, the cylinder with HWC and MNW showed no separation after reaching the maximum tensile strength.
- SEM images showed that ITZ between cement paste and 30% MNW revealed good bond efficiency, thereby developing compressive strength.
- The increased ratios of the linear attenuation coefficient for HWC were 8.8, 16.9, 24.3, and 32.4% for M-10 MNW, M-20 MNW, M-30 MNW, and M-40 MNW, respectively, at a photon energy of 0.66 MeV for ^{137}Cs. By contrast, when subjected to a photon energy of 1.33 MeV for ^{60}Co, the enhanced percentages were 12.1, 22, 28.6, and 38.5% for mixes using 10, 20, 30, and 40% MNW, respectively, due to using these MNW ratios and higher densities than the reference mix.
- However, increased MNW ratios in HWC mixes led to attenuated energy due to MNW with 59% iron (Fe), as presented in the EDX analysis. On the other hand, MNW contributes to the reduced thickness of HWC samples from 4.683 to 3.536 cm for HVL and 15.558 to 11.748 cm for TVL.
- Due to the black-grey colour of waste iron, its colour in waste iron concrete products did not change.
- This study is exploratory in nature and draws attention to the possibility of using waste iron as a concrete aggregate, which requires additional research and development.

7. Recommendations

Corrosion is an essential study issue for the durability of concrete and is recommended for future work.

Furthermore, the economic study of metal nail waste and steel slag aggregates must be analysed and compared to natural aggregates for effective cost determination.

Author Contributions: Conceptualization and methodology, M.M.A., B.A.A., M.A., I.S.A. and M.F.A.; software, validation, formal analysis, data curation, writing original draft preparation, writing review and editing and visualization, M.M.A., B.A.A., M.A., I.S.A. and M.F.A.; investigation, M.M.A., B.A.A., M.A. and M.F.A.; resources, supervision, and project administration, M.M.A., M.A., I.S.A. and M.F.A. All authors have read and agreed to the published version of the manuscript.

Funding: This research received no external funding.

Data Availability Statement: Not applicable.

Conflicts of Interest: The authors declare no conflict of interest.

References

1. Amin, M.; Abdelsalam, B.A. Efficiency of rice husk ash and fly ash as reactivity materials in sustainable concrete. *Sustain. Environ. Res.* **2019**, *29*, 30. [CrossRef]
2. Ayman, H.H.K.; Heniegal, A.; Attia, M.M. Behavior of post-tensioned fibrous lightweight concrete beams made of natural pumice. In Proceedings of the Sustainable Construction and Project Management Sustainable Infrastructure and Transportation for Future Cities, Aswan, Egypt, 16–18 December 2018.

3. Attia, M.M.; Shawky, S.M.M. Banana fiber reinforced concrete: A review. *N. Y. Sci. J.* **2021**, *14*, 48–55.
4. Rashad, A.M. A preliminary study on the effect of fine aggregate replacement with metakaolin on strength and abrasion resistance of concrete. *Constr. Build. Mater.* **2013**, *44*, 487–495. [CrossRef]
5. Rodrigues, P.; Silvestre, J.D.; Flores-Colen, I.; Viegas, C.A.; Ahmed, H.H.; Kurda, R.; de Brito, J. Evaluation of the Ecotoxicological Potential of Fly Ash and Recycled Concrete Aggregates Use in Concrete. *Appl. Sci.* **2020**, *10*, 351. [CrossRef]
6. Zega, C.J.; Di Maio, A.A. Recycled concretes made with waste ready-mix concrete as coarse aggregate. *J. Mater. Civil Eng.* **2011**, *23*, 281–286. [CrossRef]
7. *EN 206-1:2003*; Concrete-Part 1: Specification, Performance, Production and Conformity. Slovenski Inštitut za Standardizacijo: Ljubljana, Slovenija, 2000.
8. Ouda, A.S. Development of high-performance heavy density concrete using different aggregates for gamma-ray shielding. *Prog. Nuclear Energy* **2015**, *79*, 48–55. [CrossRef]
9. Devi, V.S.; Gnanavel, B.K. Properties of concrete manufactured using steel slag. *Procedia Eng.* **2014**, *9*, 95–104. [CrossRef]
10. Binici, H.; Aksogan, O.; Sevinc, A.H.; Kucukonder, A.J.C. Mechanical and radioactivity shielding performances of mortars made with colemanite, barite, ground basaltic pumice and ground blast furnace slag. *Constr. Build. Mater.* **2014**, *50*, 177–183. [CrossRef]
11. Nedeljkovic, M.; Visser, J.; Valcke, S.; Schlangen, E. Physical Characterization of Dutch Fine Recycled Concrete Aggregates: A Comparative Study. Multidiscip. *Digit. Publ. Inst. Proc.* **2019**, *34*, 7.
12. Abdel-Gawwad, H.A.; Mohammed, M.S.; Zakey, S.E. Preparation, performance, and stability of alkali-activated-concrete waste-lead-bearing sludge composites. *J. Clean. Prod.* **2020**, *259*, 120924. [CrossRef]
13. Bobrowicz, J.; Chyliński, F. Comparison of pozzolanic activity of ilmenite mud waste to other pozzolans used as an additive for concrete production. *J. Therm. Anal. Calomir.* **2021**, *143*, 2901–2909. [CrossRef]
14. Naik, T.R. Sustainability of Concrete Construction. *Am. Soc. Civil Eng.* **2008**, *13*. [CrossRef]
15. Anshassi, M.; Laux, S.J.; Townsend, T.G. Approaches to integrate sustainable materials management into waste management planning and policy. *Resour. Conserv. Recycl.* **2019**, *148*, 55–66. [CrossRef]
16. United States Environmental Protection Agency. Advancing Sustainable Materials Management. Fact Sheet. 2017. Available online: https://www.epa.gov/facts-and-figures-about-materials-waste-and-recycling/advancing-sustainable-materials-management (accessed on 6 May 2017).
17. Sear, L. Towards zero waste. *Concrete* **2005**, *39*, 50–52.
18. Bai, J.; Kinuthia, J.; Tann, D. Concrete materials research for sustainable development. *Concrete* **2005**, *39*, 37–39.
19. Neville, A.M. *Properties of Concrete*; Longman: London, UK, 1995.
20. Rakshvir, M.; Barai, S.V. Studies on recycled aggregates-based concrete. *Waste Manag. Res.* **2006**, *24*, 225–233. [CrossRef]
21. Tayeh, B.A.; Saffar, D.M.A. Utilization of waste iron powder as fine aggregate in cement mortar. *J. Eng. Res. Technol.* **2018**, *5*, 22–27.
22. Agwa, I.S.; Omar, O.M.; Tayeh, B.A.; Abdelsalam, B.A. Effects of using rice straw and cotton stalk ashes on the properties of lightweight self-compacting concrete. *Constr. Build. Mater.* **2020**, *235*, 117541. [CrossRef]
23. Maslehuddin, M.; Sharif, A.M.; Shameem, M.; Ibrahim, M.; Barry, M.S. Comparison of properties of steel slag and crushed limestone aggregate concretes. *Constr. Build. Mater.* **2003**, *17*, 105–112. [CrossRef]
24. Yang, S.; Mo, L.; Deng, M. Effects of ethylenediamine tetra-acetic acid (EDTA) on the accelerated carbonation and properties of artificial steel slag aggregates. *Cement Concrete Compos.* **2021**, *118*, 103948. [CrossRef]
25. Chunlin, L.; Kunpeng, Z.; Depeng, C.J. Possibility of concrete prepared with steel slag as fine and coarse aggregates: A preliminary study. *Proced. Eng.* **2011**, *24*, 412–416. [CrossRef]
26. Miah, M.J.; Patoary, M.M.H.; Paul, S.C.; Babafemi, A.J.; Panda, B. Enhancement of mechanical properties and porosity of concrete using steel slag coarse aggregate. *Materials* **2020**, *13*, 2865. [CrossRef] [PubMed]
27. Saxena, S.; Tembhurkar, A.R. Impact of use of steel slag as coarse aggregate and wastewater on fresh and hardened properties of concrete. *Construct. Build. Mater.* **2018**, *165*, 126–137. [CrossRef]
28. Wang, Q.; Shi, M.X.; Zhang, Z.Q. Hydration properties of steel slag under autoclaved condition. *J. Therm. Anal. Calorim.* **2015**, *120*, 1241–1248. [CrossRef]
29. Hulthen, S.I. Five decades of iron powder production. *Inf. J. Powder Metall. Powder Technol.* **1981**, *17*, 81–106.
30. Ghannam, S.; Najm, H.; Vasconez, R. Experimental study of concrete made with granite and iron powders as partial replacement of sand. *Sustain. Mater. Technol.* **2016**, *9*, 1–9. [CrossRef]
31. Ghailan, A.H. Modified concrete by using a waste material as a coarse aggregate. In Proceedings of the Construction Research Congress, San Diego, CA, USA, 5–7 April 2005; pp. 217–226.
32. Ismail, Z.Z.; Al-Hashmi, E.A. Reuse of waste iron as a partial replacement of sand in concrete. *Waste Manag.* **2008**, *28*, 2048–2053. [CrossRef]
33. Adeyanju, A.; Manohar, K. Effects of Steel Fibers and Iron Filings on Thermal and Mechanical Properties of Concrete for Energy Storage Application. *J. Miner. Mater. Charact. Eng.* **2011**, *10*, 1429–1448. [CrossRef]
34. *ASTM C150/C150M-17*; Standard Specification for Portland Cement. ASTM International: West Conshohocken, PA, USA, 2017.
35. *ASTM C33/C33M*; Standard Specification for Concrete Aggregates. ASTM International: West Conshohocken, PA, USA, 2013.
36. *ASTM C494*; Standard Specification for Chemical Admixtures for Concrete. ASTM International: West Conshohocken, PA, USA, 2013.

37. *ASTM C143/C143M-15a*; Standard Test Method for Slump of Hydraulic-Cement Concrete. ASTM International: West Conshohocken, PA, USA, 2015. [CrossRef]
38. *ESS 1658/2008*; Testing of Concrete. Egyptian Organization for Standards & Quality: Cairo, Egypt, 2008.
39. *ASTM C496/C496M-17*; Standard Test Method for Splitting Tensile Strength of Cylindrical Concrete Specimens. American Society for Testing and Materials: West Conshohocken, PA, USA, 2017. [CrossRef]
40. *ASTM C469/C469M-14*; Standard Test Method for Static Modulus of Elasticity and Poisson's Ratio of Concrete in Compression. American Society for Testing and Materials: West Conshohocken, PA, USA, 2014. [CrossRef]
41. Mostofinejad, D.; Reisi, M.; Shirani, A. Mix design effective parameters on c-ray attenuation coefficient and strength of normal and heavyweight concrete. *Constr. Build. Mater.* **2012**, *28*, 224–229. [CrossRef]
42. Gökçe, H.S.; Öztürk, B.C.; Füsun Çamb, N.; Andiç-Çakır, Ö. Gamma-ray attenuation coefficients and transmission thickness of high consistency heavyweight concrete containing mineral admixture. *Cement Concr. Compos.* **2018**, *92*, 56–69. [CrossRef]
43. Ouda, A.S.; Abdel-Gawwad, H.A. The effect of replacing sand by iron slag on physical, mechanical and radiological properties of cement mortar. *HRBC J.* **2017**, *13*, 255–261. [CrossRef]
44. Singh, K.; Singh, H.; Sharma, V.; Nathuram, R.; Khanna, A.; Kumar, R.; Bhatti, S.S.; Sahota, H.S. Gamma-ray attenuation coefficients in bismuth borate glasses. *Nuclear Instr. Methods Phys. Res. Sec. B Beam Interact. Mater. Atoms* **2002**, *194*, 1–6. [CrossRef]
45. *ASTM C138/C138M-17a*; Standard Test Method for Density (Unit Weight), Yield, and Air Content (Gravimetric) of Concret. ASTM International: West Conshohocken, PA, USA, 2017.
46. Demirboga, R.; Gül, R. Production of high strength concrete by use of industrial by-products. *Build. Environ.* **2006**, *41*, 1124–1127. [CrossRef]
47. *ACI 318-19*; Building Code Requirements for Structural Concrete and Commentary. American Concrete Institute: Farmington Hills, MI, USA, 2019.
48. Givi, A.N.; Rashid, S.A.; Aziz, F.N.A.; Salleh, M.A.M. The effects of lime solution on the properties of SiO_2 nanoparticles binary blended concrete. *Compos. Part B Eng.* **2011**, *42*, 562–569. [CrossRef]
49. Alwaeli, M.; Nadziakiewicz, J. Recycling of scale and steel chips waste as a partial replacement of sand in concrete. *Constr. Build. Mater.* **2012**, *28*, 157–163. [CrossRef]
50. Rai, A.; Prabakar, J.; Raju, C.B.; Morchalle, R.K. Metallurgical slag as a component in blended cement. *Constr. Build. Mater.* **2002**, *116*, 489–494. [CrossRef]
51. Tufekci, M.M.; Gokce, A. Development of heavyweight high-performance fiber reinforced cementitious composites (HPFRCC)–Part II: X-ray and gamma radiation shielding properties. *Constr. Build. Mater.* **2018**, *163*, 326–336. [CrossRef]
52. Saad, M.; Agwa, I.S.; Abdelsalam Abdelsalam, B.; Amin, M. Improving the brittle behavior of high strength concrete using banana and palm leaf sheath fibers. *Mech. Adv. Mater. Struct.* **2020**, *29*, 1–10. [CrossRef]
53. *ACI 318-08*; Building Code Requirements for Structural Concrete and Commentary. American Concrete Institute: Farmington Hills, MI, USA, 2008.
54. Akkurt, I.; El-Khayatt, A.M. The effect of barite proportion on neutron and gamma-ray shielding. *Ann. Nuclear Energy* **2013**, *51*, 5–9. [CrossRef]
55. Lotfi-Omran, O.; Sadrmomtazi, A.; Nikbin, I.M. A comprehensive study on the effect of water to cement ratio on the mechanical and radiation shielding properties of heavyweight concrete. *Constr. Build. Mater.* **2019**, *229*, 116905. [CrossRef]
56. Özen, S.; Şengül, C.; Erenoğlu, T.; Çolak, Ü.; Reyhancan, I.A.; Taşdemiŕ, M.A. Properties of heavyweight concrete for structural and radiation shielding purposes. *Arab. J. Sci. Eng.* **2016**, *41*, 1573–1584. [CrossRef]
57. Roslan, M.K.A.; Ismail, M.; Kueh, A.B.H.; Zin, M.R.M. High-density concrete: Exploring Ferro boron effects in neutron and gamma radiation shielding. *Constr. Build. Mater.* **2019**, *215*, 718–725. [CrossRef]